



Detection of floating plastics from satellite and unmanned aerial systems (Plastic Litter Project 2018)



Konstantinos Topouzelis^{a,*}, Apostolos Papakonstantinou^b, Shungudzemwoyo P. Garaba^c

^a Department of Marine Science, University of the Aegean, University Hill, 81100, Mytilene, Greece

^b Department of Geography, University of the Aegean, University Hill, 81100, Mytilene, Greece

^c Institute for Chemistry and Biology of the Marine Environment-Terramare, Carl von Ossietzky University of Oldenburg, Schleusenstraße 1, 26382 Wilhelmshaven, Germany

ARTICLE INFO

Keywords:

Marine litter
Marine debris
UAV
Drone
Sentinel-2

ABSTRACT

A rapidly rising amount of plastic litter on land and at sea is becoming a global wicked environmental problem. Here, we present an innovative exploratory application of unmanned aerial systems (UAS) and open-access satellite imagery in remote detection of floating plastics in natural seawater, through a dedicated aquatic environment experiment. We aimed to extract meaningful spectral measurements in near-real scenarios and to compare the geospatial information ranging from moderate to very high resolution. A set of three artificial floating plastic targets were setup for remote detection in the waters close to Tsamakia beach of Mytilene on Lesvos Island, Greece. These floating targets consisted of 100 m² PET-1 1.5 L water bottles, LDPE plastic bags and nylon fishing ghost nets. Spectral properties of the controlled targets as well as surrounding seawater were investigated for Sentinel-2A satellite data. We demonstrate how UAS very high geospatial resolution images can be useful in improving geo-referencing of satellite images and how UAS can be used to assess the plastic percentage coverage of satellite images. We observed very weak to strong relationships between percentage pixel coverage and the spectral reflectance at *p*-value < 0.1 significance level. Effects of atmospheric correction algorithms was evaluated using Sen2Cor and ACOLITE, derive unbiased percentage differences were less than 65%. Our feasibility study demonstrated the importance of very high geo-spatial resolution UAS datasets in validating and enhancing the geo-spatial accuracy of satellite data for monitoring plastics in the aquatic environment. Monitoring and identifying plastics needs an integrated suite of sensors, we therefore present how available tools can be utilized to improve current efforts and contribute to advancing relevant future remote sensing technologies.

1. Introduction

Plastics pose a considerable threat to the livelihood of the aquatic species and ecosystems as they can transport bio-accumulative harmful pollutants over long time intervals (Colton et al., 1974; Rezania et al., 2018; Thevenon et al., 2014). Toxic smaller sized ocean plastics can be easily mistaken for food and hence can be transferred across aquatic vertebrates and invertebrates (Ivar do Sul and Costa, 2014). As for the larger sized pieces like ghost nets, these have been found to be responsible for large amounts of accidental by-catch of pelagic species, seabirds, turtles or even cetaceans (Thevenon et al., 2014). In the last years, a number of initiatives have been started within the framework of cleaning, recycling and curbing the plastic pollution challenge. More recently, there was a G20 meeting in Germany that brought together world leaders and stakeholders linked by the Global Partnership on

Marine Litter of United Nations Environment Programme, where they came up with an action plan on marine litter (G20, 2017). The G20 action plan echoed the need for innovative, affordable and sustainable approaches to better monitor, reduce and manage plastics in the aquatic environment.

Unmanned Aerial Systems (UAS) offer affordable ‘above-the-head’ monitoring allowing wide area coverage and very high geospatial resolution collection of information (Colomina and Molina, 2014). This means UAS, aircraft and satellites have the capability to complement ocean surface net trawl datasets of marine litter (Garaba et al., 2018; Mace, 2012; Maximenko et al., 2016). Near to shortwave infrared (NIR-SWIR) imaging from airborne and spaceborne platforms is now widely foreseen to be an upcoming source of supplementary information with a wide spatial coverage for detecting and tracking aquatic plastics. Already, efforts to use remote sensing for plastic detection have been

* Corresponding author.

E-mail addresses: topouzelis@marine.aegean.gr (K. Topouzelis), apapak@geo.aegean.gr (A. Papakonstantinou), shungu.garaba@uni-oldenburg.de (S.P. Garaba).

showing promising results with an increasing number of works demonstrating reasonable detection and mapping potential over water as well as on land (Aoyama, 2016; Garaba et al., 2018; Garaba and Dierssen, 2018; Hörig et al., 2001; Novelli and Tarantino, 2015; Veenstra and Churnside, 2012). Furthermore, the scientific community and national space agencies are working towards the specifications of satellite mission relevant for detecting and quantifying marine plastic litter.

For the first time, a project named “Plastic Litter Project 2018: Drone Mapping and Satellite Testing for Marine Plastic on the Aegean Sea” (PLP18) was conducted to explore the feasibility of detecting plastics in the aquatic environment using geoinformation acquired from unmanned aerial systems (UAS) and open access satellite missions. In the framework of this project, we aimed to extract meaningful spectral measurements in near-real scenarios and to compare the geospatial information ranging from moderate to very high resolution. The initial objective of this experiment was to examine the visibility of the plastic targets from the Copernicus Sentinel-2 satellite and to simulate the coarse satellite pixel using the fine UAS resolution. An evaluation of the different observing platforms was also completed as a step towards future directions in remote sensing of plastics.

2. Materials and methods

Our controlled experiment was conducted on 06 and 07 June 2018 close to Tsamakia beach of Mytilene on Lesvos Island, Greece (Fig. 1). A trial run based on our plan of action was completed on 06 June 2018 followed by the fine-tuned execution of the experiment on 07 June 2018. Tsamakia beach stretches for about 400 m in length with pristine nearshore waters. The top layer of the beach is sandy mixed with some pebbles and the deeper waters are covered by *Posidonia oceanica* seagrass meadows. The seagrass was used to provide an additional dark target since the open ocean water is a dark target with low reflectance in the NIR and SWIR wavelength ranges. Weather conditions during the experiment were ideal; clear skies, very calm sea conditions (1–2 cm of

waves, no visible white caps) and with low wind speed (2 m/s). Scattered cloud cover was observed in the northern part of just outside our study region.

2.1. Plastic target material

The controlled targets used in PLP18 were (i) plastic bottles, (ii) plastic bags and (iii) plastic fishing net (Fig. 1). Each one of these targets was held together by a 10 x 10 m frame, matching the Sentinel-2 spatial resolution. PVC pipes with a 2-inch diameter were used to construct the frame and plastic net with 1.5 cm mesh size was attached to create the base of the frame. The frame construction was essential for the experiment as to prevent plastics loss by a possible sinking of samples. The three targets were positioned at least 30 m away from the coastline to mitigate adjacency and mixed pixel detection from spaceborne data. However, the plastic bags target placed it partially above the sand substrate and partly above seagrass meadows. The full deployment of all the three targets was materialized with the assistance of about 30 students, divers and inflatable boats at 08:00 UTC (11:00 local time) and removed at 17:30 UTC (20:30 local time) just after Sentinel-1 satellite overpass.

A total of 3600 polyethylene terephthalate (PET-1) 1.5 l bottles were arranged into 120 strips of 30 bottles each to construct the first target. Fishing line was used to attach the bottles in line and a wooden stop every 10 bottles was tied to provide bottle stability. Labels on the bottles were not removed, but the uncovered parts were transparent. The closed bottles were empty, not filled with any fluid, but some little amount of seawater trickled in through the holes that were used for fishing line during the experiment. The second target was made up of 138 large blue coloured low-density polyethylene (LDPE) bags. The bags were attached to the PVC frame using a thin fishing line and they covered the total area of the frame. The frame made it possible to keep the plastics afloat although some portions were slightly submerged. The third target was constructed using 200 m² of abandoned yellowish nylon fishing nets. We considered this net as a representative example



Fig. 1. True colour R (590–670) nm, G (500–590) nm, B (455–515) nm composite image from a Planet® Dove satellite captured on 07 June 2018. Floating targets of blue plastic bags, yellow fishing net and clear water bottles captured by a Sony A5100 24.3-megapixel camera integrated on a S900 DJI hexacopter UAS (inset highlighted in red) over Tsamakia beach, Greece (For interpretation of the references to colour in this figure legend, the reader is referred to the web version of this article).

of a ghost net. The fishing net was attached to a white plastic net using fishing line, but without being able to cover all the white background. Furthermore, the optical density of the fishing net was not homogenous providing a near representation of a slightly submerged ghost net. During the experiment, we assumed the contribution by the background material of the net was negligible for analyses conducted in this study. These materials were chosen based on prior reports indicating types of plastics common in marine litter as well as land based litter (PlasticsEurope, 2018; Thevenon et al., 2014).

2.2. Unmanned aircraft system (UAS)

A suite of small light weight cameras or imagers were attached to a S900 DJI hexacopter (S900-UAS) capable of a 25-minute flight time with a payload of 1.5 kg. S900-UAS geolocation information was recorded by a differential global positioning system. Among the sensors was a 0.224 kg interchangeable Sigma ART 19 mm 1:2.8 DN0.2 M/0.66Feet 46 lens Sony A5100 24.3-megapixel camera capable of precise autofocus in 0.06 s, captured high quality true colour RGB images. A custom-made multispectral SLANTRANGE 3 P (S3 P) sensor with an integrated global positioning system/inertial measurement unit system as well as ambient illumination sensor for deriving spectral reflectance-based end-products was also attached to the S900-UAS. The S3 P has a quad-core 2.26 GHz processor and a 2 GB RAM embedded. The wavebands were adjusted to match the coastal, blue, green and NIR wavebands on the Sentinel-2 mission (Table 1). Waveband adjustment to S3 P imager were aimed at simulating Sentinel-2 data in finer geospatial resolution by capturing the features in the deeper water layer, useful in investigating pixel interaction from very fine (cm) to coarse (tens of meters) resolution. A compact Parrot Sequoia (PS) multispectral camera weighing 135 g was also used to collect spectral information from four narrow wavebands (green, red, red edge and NIR) equipped with a global positioning system. Thermal imagery was acquired using a compact 84 g FLIR Duo R camera with 160 × 120 thermal sensor and 1920 × 1080 visible optical pixel resolution.

A trial aerial survey was conducted on 06 June 2018 using the S900-UAS to assess sensor suite, prepare and adapt any necessary settings for final flight plan. On 07 June 2018, very fine resolution imagery (3–5) cm was autonomously collected over an area covering ~206,390 m² by the S900-UAS. Flight altitude was set at 100 m above sea water with an 85% overlap of the aerial images and an 80% sidelap for the S3 P internal sensor parameters. Two surveys were completed on 07 June 2018 each lasting ~13.5 min thus capturing in total 2846 very fine geospatial resolution images although the ground sampling resolution was different (Table 2). Ground sampling resolution varied due to the focal length, pixel pitch and sensor size of the imagers used. The finest ground sample distance calculated was 2.14 cm/pixel for the Sony A5100 camera (Table 2).

True colour orthorectified images were generated from the S3 P, PS and Sony A5100 RGB cameras (Table 2). No further processing was done for the FLIR Duo R imagery because it was captured at a relatively coarser pixel resolution greater than 10 cm/pixel. UAS spatial data acquisition and the Structure from Motion (SfM) photogrammetric

Table 1

Waveband information for the SLANTRANGE 3 P imager and Sentinel-2 missions. Coastal (C), blue (B), green (G), near infrared (NIR).

SLANTRANGE 3 P		Sentinel-2 A		Sentinel-2B	
Centre (nm)	Bandwidth (nm)	Centre (nm)	Bandwidth (nm)	Centre (nm)	Bandwidth (nm)
C 450	20	442.7	27	442.2	45
B 500	80	492.4	98	492.1	98
G 550	40	559.8	45	559.0	46
NIR 850	100	832.8	145	832.9	133

Table 2

Number of raw images and geo-spatial resolution acquired using a suite of sensors attached to a S900-UAS.

Name of Sensor	Number of Images	Resolution (cm/pixel)
SLANTRANGE 3 P	394	4.84
Parrot Sequoia multispectral	872	7.73
Parrot Sequoia RGB	187	2.72
Sony A5100	243	2.14
FLIR DUO R Thermal	575	196.50
FLIR DUO R Visible	575	10.53

pipeline was implemented for orthophoto production. SfM pipeline is based on computer vision image processing algorithms. Here it was automated to generate very high geo-spatial resolution orthophotos of Tsamakia beach and floating targets. This followed pipeline using the overlapping sequences of two-dimensional images was used to produce orthophotos and digital surface models DSM as previously done in prior works (Cook, 2017; Doukari et al., 2016; Eltner et al., 2015; Mancini et al., 2013; Papakonstantinou et al., 2016; Tonkin et al., 2014).

The orthophotos were produced in Agisoft Photoscan Professional Edition version 1.4.4. Geo-referencing of the Sony A5100 orthophotos was achieved using 7 ground control points (GCPs) having a total root mean square error of 0.244 cm. The two multispectral orthophotos from S3 P and PS were then georeferenced by utilizing the georeferenced Sony A5100 orthophoto as a base map. An inter-comparison of the three georeferenced orthophoto maps was completed to best match common characteristic reference points. Final end-products consisted of georeferenced orthophotos (i) S3 P – coastal (450 nm), blue (500 nm), green (550 nm) and NIR (850 nm) (ii) PS – green (550 nm), red (660 nm), red edge (735 nm) and NIR (790 nm) (iii) PS optical true colour RGB and (iv) Sony A5100 in optical true colour RGB. False colour composite images were produced for the multispectral sensor without RGB wavebands i.e. PS (R = 660 nm, G = 735 nm, B = 790 nm) and S3 P (R = 550 nm, G = 500 nm, B = 450 nm).

2.3. Satellite data

Satellite imagery acquired over Tsamakia beach on 07 June 2018 by the Copernicus Sentinel missions was retrieved from the Copernicus Open Access Hub (<https://scihub.copernicus.eu/>). An image was captured by Sentinel-2A multispectral instrument at 08:56 UTC or 11:56 local time and an additional image was taken by Sentinel-1 at 16:07 UTC or 19:07 local time (Table 3). Sentinel-1 Synthetic Aperture Radar (SAR) image was captured in interferometric wide swath mode, covering a 250 km swath at 5 m by 20 m spatial resolution – single look.

Standard Sentinel-2 Level 1C and Level 2A (nominal values) products were analysed using the European Space Agency software Sentinel Application Platform (SNAP) version 6.0.0. The Sentinel-2A image was resampled to 10 m spatial resolution. The region of interest was then obtained by cropping thus reducing image size and processing time. Furthermore, a land mask was applied to the cropped-out image as our study was focussed on seawater floating targets. Spectral information was retrieved from pixels corresponding to the three plastic targets as well as surrounding seawater. The pixels representing water were identified as the optically deep portions of the water minimizing bottom reflectance. An additional atmospheric correction approach was

Table 3

List of Sentinel images captured on 07 June 2018 over Tsamakia beach of Mytilene on Lesvos Island, Greece.

Image Filename
S1A_IW_SLC_1SDV_20180607T160715_20180607T160742_022253_02686F_1B45
S2A_MSIL1C_20180607T085601_N0206_R007_T35SMD_20180607T110513
S2A_MSIL2A_20180607T085601_N0208_R007_T35SMD_20180607T114919

applied to the Level 1C image to generate a Level 2 image with (band averaged values) inter-comparison purposes using ACOLITE version 20,180,925 (Vanhelmont and Ruddick, 2018). We did not have a reference spectra dataset, so for comparison of the Level 2 algorithm end-products we derived the unbiased percentage differences as done previously (Garaba and Zielinski, 2013; Hooker et al., 2002).

S900-UAS imagery was compared to the Sentinel-2 images using the spectral information retrieved from the matching targets. It involved identifying spatial and spectral anomalies. The S900-UAS very high geospatial resolution (~ 0.03 m) images were used as master images for improved geo-referencing of the Sentinel-2 images (~ 10 m). Validation of the georeferencing was also completed using matching WorldView and Planet[®] Dove data. Uncertainties were not fully determined for the final Sentinel-2 image due to lack of ground control points but for brevity we assume a value of 0.5 m. Percentage pixel coverage of the plastic targets in the Sentinel-2 image and the spectral data was extracted for each pixel. Pixel coverage was determined through object-based image analysis by assuming the floating plastic targets and the water as primary end-members.

Using SNAP we also processed the Sentinel-1 image by cropping out region of interests after applying the thermal noise removal, sigma0 calibration and Terrain Observation with Progressive Scans SAR deburst algorithms. Pixel backscattering values were examined for the different plastic targets and for the various polarization options. The C-band was used to investigate the sea surface roughness on the water surface and the interaction between the small gravity-capillary waves of the water with the plastic targets.

3. Results and discussion

3.1. S900-UAS imagery

Very high geospatial resolution orthophotos were generated from the aerial survey conducted on 07 June 2018 using multiple sensors integrated on a S900-UAS. Sony A5100 RGB images were acquired at $16,887 \times 14,577$ pixels resulting in 2.14 cm/pixel resolution, PS RGB at 4608×3456 pixels size equal to 2.72 cm/pixel resolution, S3 P multispectral at 7353×6949 pixels giving a resolution of 4.84 cm/pixel and PS multispectral sensor at 5920×5366 pixels thus a resolution of 7.73 cm/pixel (Table 2 and Fig. 2).

The lens size and specifications on the Sony A5100 camera resulted in high quality orthophotos thus improved the georeferencing process of the additional imagery from the PS and S3 P sensors. A reasonable amount of surface reflected glint was observed in the orthophotos although efforts to mitigate inherent effects were made including having the flight plan slightly heading away from the sun. However, at midday 12:00 the sun was overhead and avoiding glint was challenging especially without automated or real-time image visualization to adjust flight settings (Fig. 2a and b). In all the images it was clear that the land targets were brighter and as we moved offshore with increasing water depth, we ended up with darker less reflective targets primarily water. Water is a strong light absorber in the NIR to SWIR wavelengths (Kou et al., 1993). The false colour composites from the multispectral imagery of the PS and S3 P exhibited the potential to visually distinguish the floating targets (Fig. 2c and d). The PS false colour image (NIR wavebands) showed a darkening of the image offshore except for the floating plastic targets (Fig. 2c). An assessment of the thermal imagery did not reveal significant variations when we compared the water surface and the three plastic targets. As expected, the land targets were warmer than the vegetation and the water targets, a transition zone was noted to be the yellow region which was the edge of the bright land or cool water (Fig. 2e). A qualitative visual inspection of the thermal image suggests only the plastic bottles and the plastic bags were detected with some degree of uncertainty. This could be because the bottles were well aggregated, empty and floating meaning moderate temperature due to cooling by the water and heating by sea reaching

solar energy (Fig. 2e), the same could apply to the blue plastic bags. Furthermore, for the plastic bottles there is a chance of a small greenhouse effect caused by the empty bottles, as they have capability to retain thermal radiation inside them, whilst the other targets did not have an empty space to create a detectable thermal target. Additionally, the thermal sensitivity of our FLIR DUO R thermal imager at ~ 1.97 m geospatial resolution might not have been optimal for resolving temperature variations over a dark target like water, something to be explored in a follow up investigation. The RGB orthophotos demonstrate the benefits of very high geospatial resolution imagery as the beach basin features (hard rocky, sand, seagrass covered) and land-based structures (vegetation, buildings, roads, pier, beach umbrellas, soccer pitch) can be distinguished (Fig. 2f).

3.2. Sentinel-2A satellite optical imagery

The three targets were detected in the Sentinel-2 true colour composite image ($R = 665$ nm, $G = 560$ nm, $B = 490$ nm) collected on 07 June 2018 (Fig. 3). Greyscale images at discrete wavebands (490, 560, 665 and 842 nm) also suggests that the bright floating targets can be detected from space. The blue plastic bags are an exception as they were not easy to distinguish in the green and red waveband imagery (insets Fig. 3).

All targets are observed in the NIR waveband (842 nm) as expected because plastics have a distinct optical signature in these waveband, consistent with previous studies (Cloutis, 1989; Garaba and Dierssen, 2018; Huth-Fehre et al., 1995). The clear bottles and white fishing net targets are expected to have a high nearly flat signal in the visible spectrum and therefore are salient in the RGB wavebands. Optical properties of clear, beige, ivory and white coloured plastics have been reported to be reflective with a generally flat signal in the visible spectrum (Garaba and Dierssen, 2018). Therefore, the blue plastic bags as expected had a peak in the blue wavelengths that decreased towards the green and red wavebands. The reflectance increased in the NIR spectrum a typical optical characteristic of plastics.

To quantitatively assess the targets we looked at the spectra after deriving percentage pixel coverages. Each target ended up covering 4 adjacent pixels after geometric and resampling corrections using the Sony A5100 very high geospatial resolution imagery as master input (Fig. 4). A high pixel percentage coverage was associated with a high reflectance, at nearly all with the exception of the fishing nets, of the observed wavebands. A weak degree of correlation at lower percentage pixel coverages of the fishing nets to the reflectance in the visible and NIR spectrum might be due to bottom reflectance dominating the bulk spectral signature observed. Indeed, it will be crucial for future studies to collect auxiliary in-situ measurements of other optically active constituents of target waters thus making it possible to better decompose the bulk spectral signature. Spearman rank-order correlation tests indicated very weak to very strong positive correlations at $p\text{-value} < 0.1$ significance level, with the exception of individual wavebands with negative correlations e.g. 443 nm. Although we do not explore quantification of the plastics using spectral unmixing approaches here, ongoing work is exploring the use of Sentinel-2 datasets in quantifying floating plastics in various aquatic environments. Furthermore, here we observed the spectral reflectance of the floating plastic detected by Sentinel-2 A was reasonably correlated to the percentage pixel coverage of each target, suggesting potential application of spectral unmixing algorithms in future efforts to quantify and detect floating plastics. Of course, implementing spectral unmixing methods would require knowledge of other end-members in waters of interest or use of spectral reference libraries.

Top-of-atmosphere spectra of the primary targets was higher than the bottom-of-atmosphere products as expected (Fig. 5a). However, it was observed that the standard Sen2Cor end-products had a higher reflectance compared to ACOLITE products (Fig. 5b–e). Unbiased percentage differences at different wavebands and each target varied

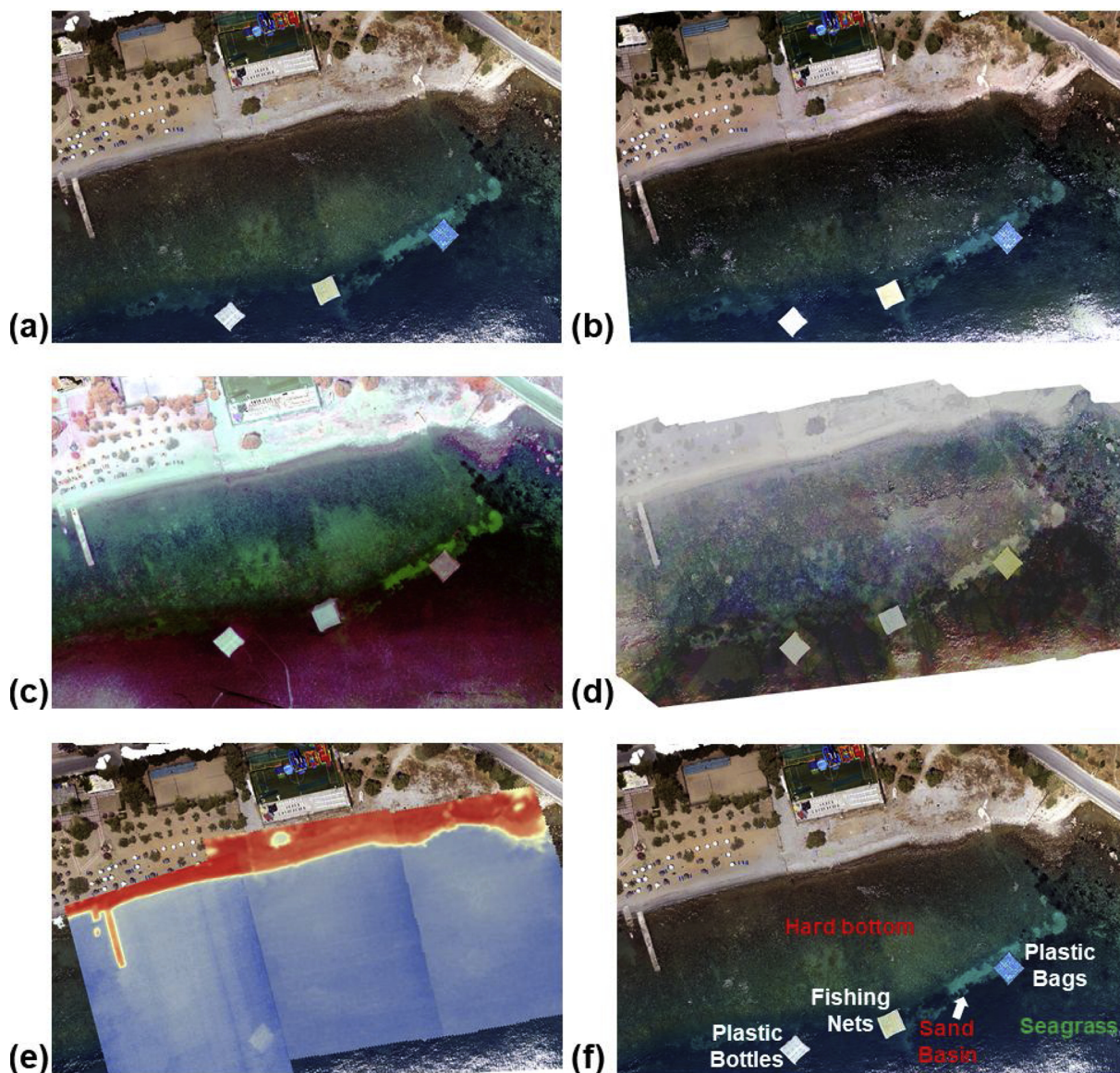


Fig. 2. Very high geospatial resolution orthophotos (a) Sony A5100, (b) PS for true colour RGB composite, (c) PS and (d) S3 P multispectral cameras false colour composite, (e) FliR DUO R thermal mosaic overlaid on a Sony A5100 and (f) Sony A5100 highlighting the different targets in the water captured using a S900-UAS on 07 June 2018 over Tsamakia beach, Greece.

between 1% to 64% (Table 4). These differences were lowest in the NIR (740–865) nm ranging from 1% to 21% but highest in the SWIR (1610–2190) greater than 35%. Spectrally all plastic targets were easy to distinguish from the water target due to the higher reflectance compared to the surrounding water (Fig. 5f). Here, ACOLITE spectra were selected because of the lowest reflectance spectra output but does not mean it is the best result because no reference data is available. Furthermore, seawater is a strong light absorber in the NIR which means it should have low to little reflectance in the NIR to SWIR spectrum (Garaba et al., 2018; Kou et al., 1993). It has to be noted that ACOLITE generates waveband averaged spectra whilst Sen2Cor uses nominal waveband values, also the water absorption feature ~ 945 nm is not an output in the ACOLITE processing (Fig. 5).

However, both atmospheric correction algorithms, Sen2Cor and ACOLITE, evaluated here suggest that floating plastic can be detected, and the signal will not be masked after removing environmental perturbations in the top-of-atmosphere spectral reflectance. Follow-up studies need to further assess how other atmospheric correction approaches might change the spectral reflectance magnitude and shape.

Magnitude and shape of the signal are important features that are used in quantification, identification or detection algorithms (Keshava and Mustard, 2002; Shanmugam and SrinivasaPerumal, 2014).

Although in-situ measurements of suspended sediments, coloured dissolved organic material, algae were not gathered during the experiment it is crucial to account for them in future studies. Using hyperspectral spectroscopy in-situ measurements will be of value especially for discriminating the plastics from other bright targets such as whitecaps, floating vegetation and bottom reflectance for shallow waters with bright sediments. Algorithm tuning and development does require high quality measurements from various targets and scenarios to mitigate false positives in future monitoring applications relevant to plastics.

3.3. Sentinel-1 satellite radar imagery

An additional possible source of information relevant to plastic litter is active remote sensing using Sentinel-1 SAR imaging, an approach that is not affected by cloud cover and does not depend on ambient light.

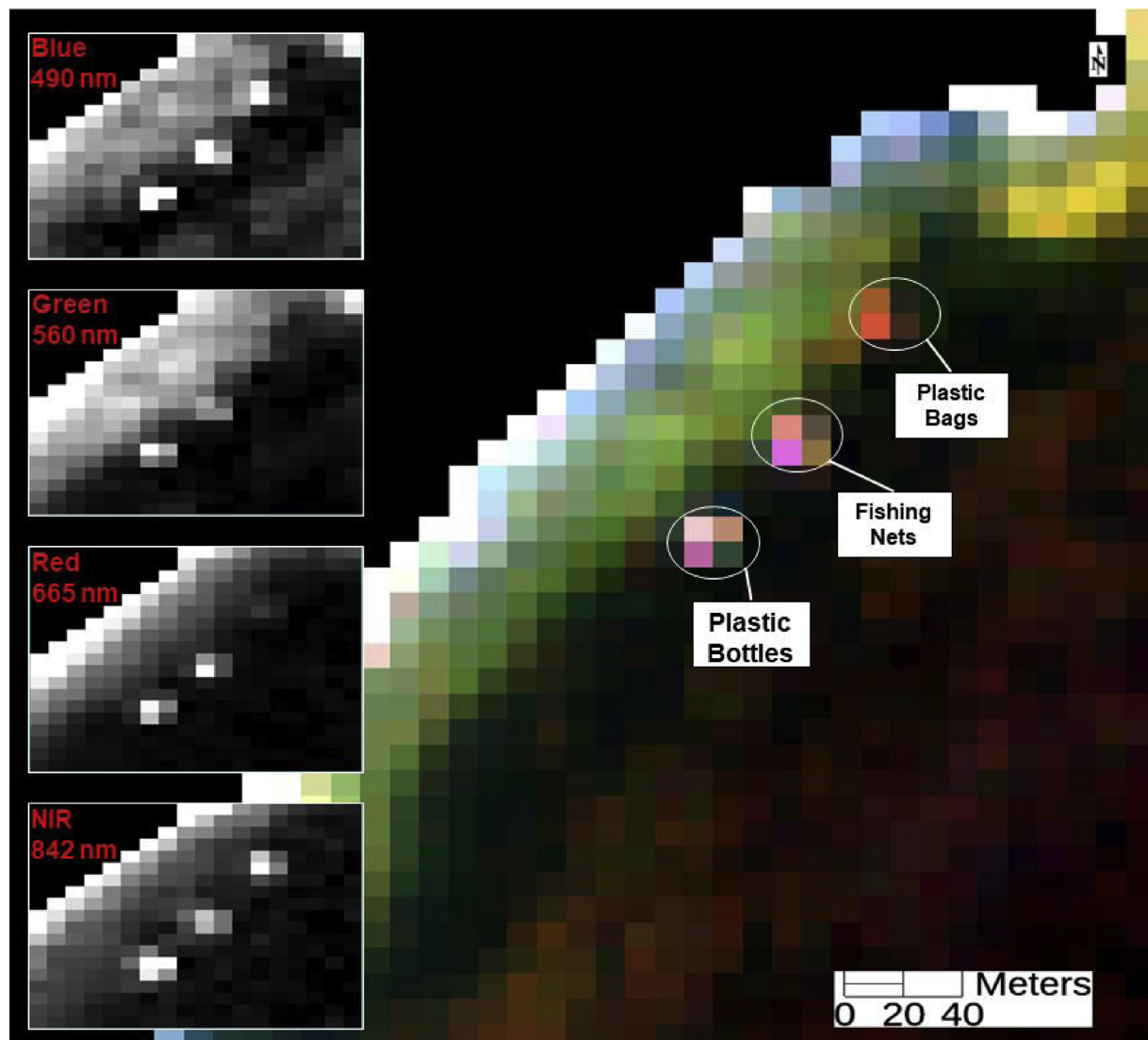


Fig. 3. A land masked Sentinel-2 A Level 2 A true colour composite ($R = 665 \text{ nm}$, $G = 560 \text{ nm}$, $B = 490 \text{ nm}$) captured on 07 June 2018 over Tsamakia beach, Greece.

The radar imagery collected on 07 June 2018 demonstrates how Sentinel-1 can be utilized in monitoring floating litter. An analysis of the derived backscatter showed variations between the plastic targets and surrounding water. A possible source of these observed differences in the backscatter could be from changes in sea state, leading to a dampening effect of the sea capillary waves. However, due to the Single Look Complex (SLC) type of the product and the very low wind condition the targets were not easily detected in the image. Of the three targets, only the plastics bottles target was noticeable in the VV polarized Sentinel-1 radar image captured (Fig. 6). The fishing nets and plastic bags were had a very low backscattering signal, similar to the clean sea. This is a result of high roughness form the plastic bottles in opposite of the low backscatter values of the surrounding sea. The opposite is expected with medium to high wind speeds where all the targets will dampen the small gravity capillary waves and will be shown

as areas with low backscatter signal i.e. darker areas in a brighter background. Further investigations are expected to look at the different wind speeds using a wider range of floating targets of varying sizes.

4. Conclusions and outlook

We demonstrate for the first time the remote sensing prospects of floating plastics from state-of-the-art UAS and spaceborne platforms. The approaches are clearly complementary and using the very high geospatial resolution imagery captured by a UAS we also show how geo-referencing of spaceborne imagery can be enhanced. We also provide reasonable evidence that both SAR and optical imagery captured by Sentinel-1 and Sentinel-2 respectively have potential application in detecting floating plastics in marine litter. Indeed, the identification of the plastic types and shapes will require multi- to hyperspectral

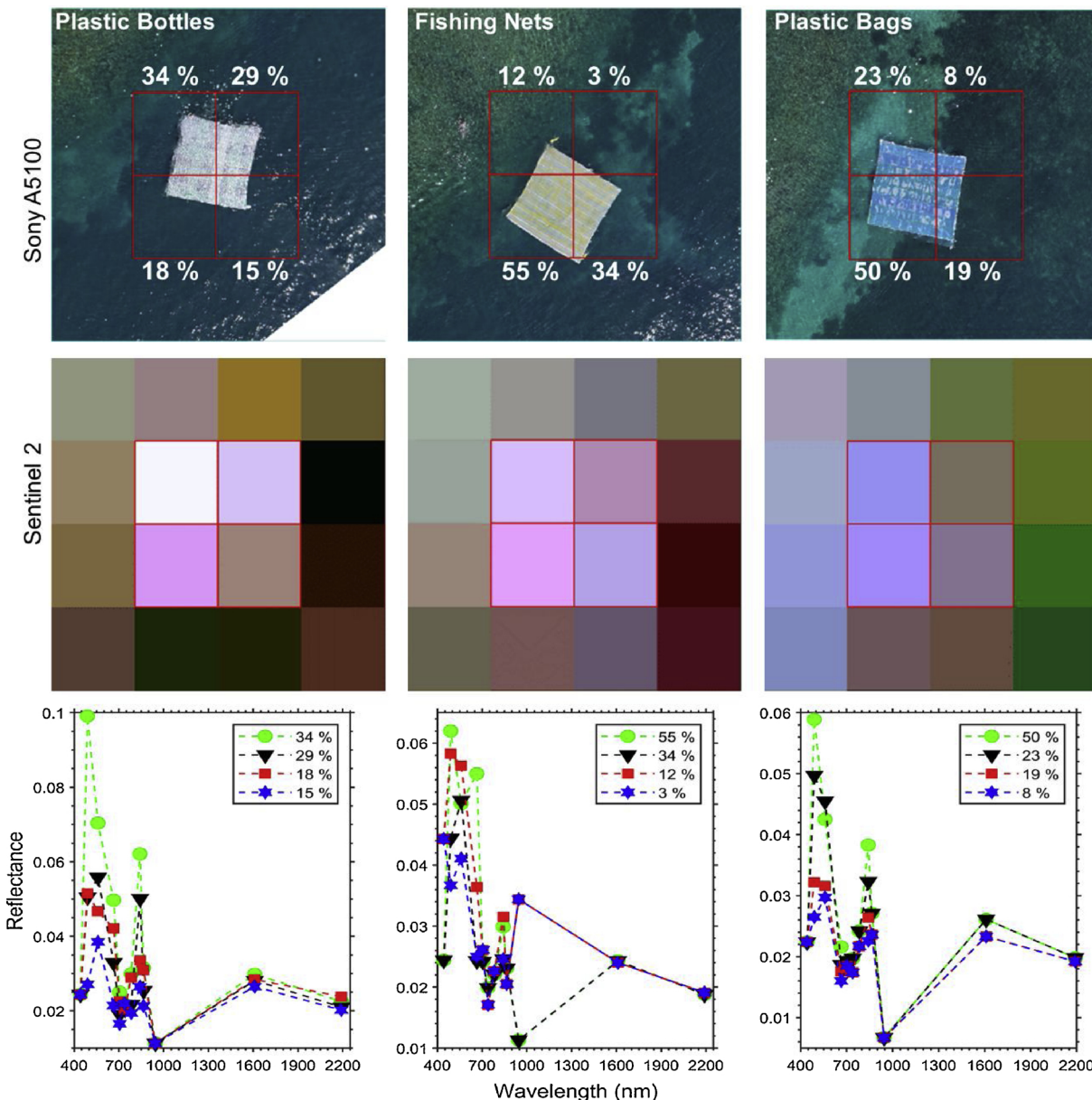


Fig. 4. Percentage pixel coverage of the floating plastic targets determined in the true colour images captured by the Sony A5100 and matching pixel spectra from the Sentinel-2 A imager.

imaging, but our current starting goal is to contribute towards optimizing current datasets or mission to be able to detect and identify plastics in marine litter.

Although UASs are a very powerful tool in monitoring plastics there are payload, power, operational costs and aviation regulation constraints that have been well documented in literature (Colomina and Molina, 2014). As remote sensing of plastic litter is still in the grassroot phase, to complement true color imaging for visual or shape detection efforts we have to be aware that current polymer identification algorithms require hyperspectral measurements of unknown plastics for higher degree of certainty matching using spectral reference libraries of

known polymers. However, integrating hyperspectral imagers on typical off-the-shelf UAS translates to a costly more power and payload capable system. Another important challenge to science plastic litter monitoring efforts is obtaining aviation licenses in various regions of interest. Ongoing and future studies need to consider developing algorithms that can operationally utilize spectral information, on affordable as well as current suite of remote sensing optical technologies, to detect and possibly distinguish plastics in marine litter. Once these approaches become robust using UAS very fine geospatial imagery, there will be a need to transfer the knowledge to current or planned satellite missions. Additionally, future efforts will involve a comparison

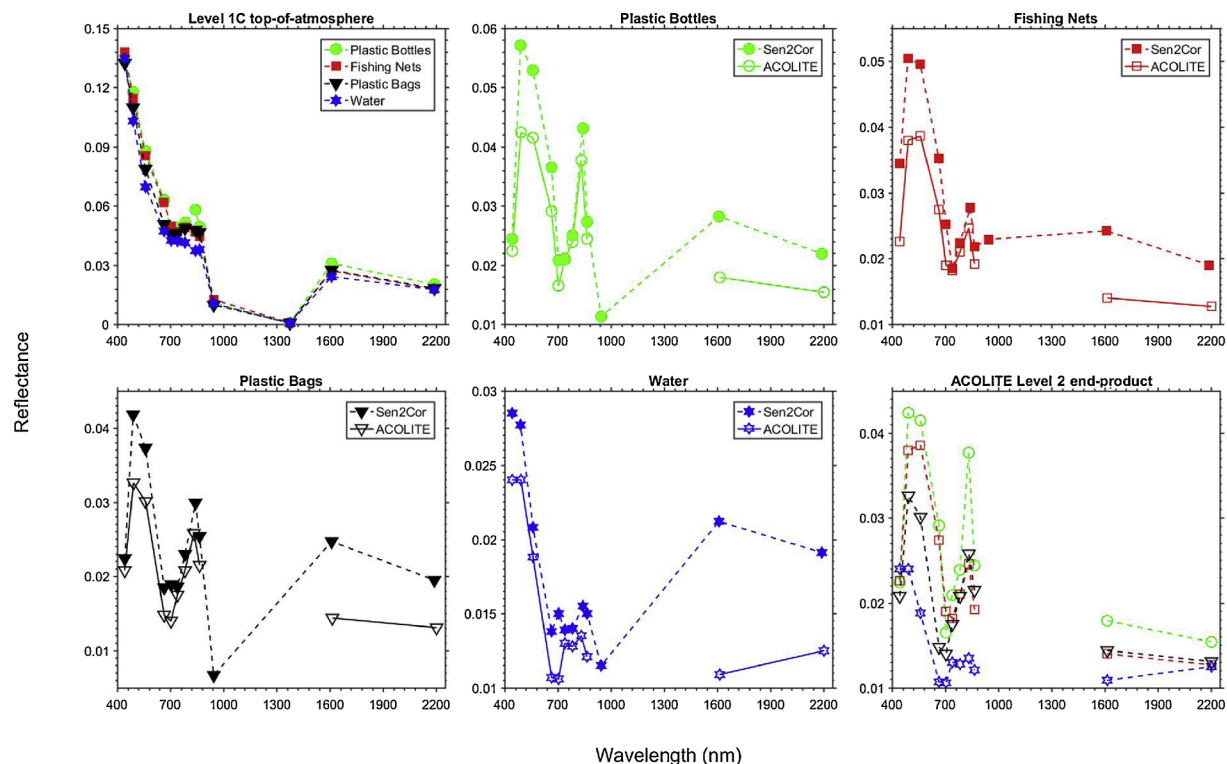


Fig. 5. Sentinel-2 A averaged bulk (a) Level 1C top-of-atmosphere reflectance of the primary targets, (b) plastic bottles target, (c) fishing nets target, (d) plastic bags target, (e) water ACOLITE and Sen2Cor Level 2 bottom-of-atmosphere corrected spectra and (f) ACOLITE corrected spectra.

Table 4

Unbiased percentage differences between ACOLITE and Sen2Cor Level 2 bottom-of-atmosphere corrected spectra of the main targets.

Wavelength (nm)	Plastic Bottles (%)	Fishing Nets (%)	Plastic Bags (%)	Water (%)
443	9	41	7	17
490	30	28	25	14
560	24	25	21	10
665	23	25	22	25
705	23	28	30	34
740	1	2	6	7
783	4	6	10	9
842	13	12	15	14
865	11	13	17	21
1610	45	53	53	64
2190	35	40	39	42

of the spectral data gathered during this study by the imagers on the S900-UAS with those from the Sentinel-2 A and other spaceborne sensors.

Atmospheric correction of imagery captured from space is a key source of information with wide geo-spatial coverage and possible temporal resolution. Although, it has been shown that there are uncertainties using Sen2Cor and ACOLITE algorithms, both end-products have a potential in the detection of floating plastics. Extensive inter-comparison campaigns using high quality in-situ measurements as reference spectral data are needed to derive error budgets as well as optimize atmospheric correction especially in different water bodies and meteorological conditions. Furthermore, results of such inter-comparisons could benefit the remote sensing community in terms of differentiating common oceanic bright targets such as plastics, white-caps, seafoam and surface reflected glint. A high-quality dataset with traceable errors of different optically active components can be utilized to generate generic end-members essential in deriving quantitative or qualitative parameters from spectral unmixing algorithms.

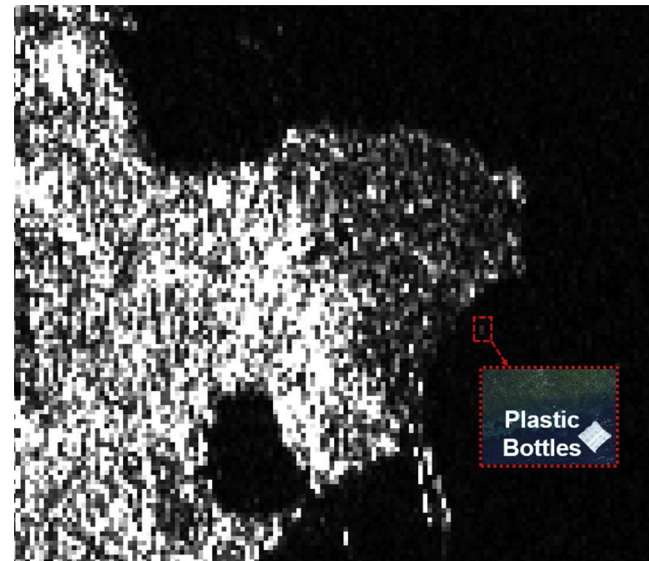


Fig. 6. Sentinel-1 SAR VV polarized greyscale imagery showing potential detection of the floating plastic bottles, RGB image inset captured on 07 June 2018 over Tsamakia beach, Greece.

Acknowledgments

We would like to thank Marine Remote Sensing Group members Michaela Doukari for helping in the orthophoto creation and data georeferencing, Andromachi Chatziantoniou for spectral analysis, Efi Konstantinidou for Sentinel-1 processing and Spyros Spondilidis for UAV data transformation. Targets construction was completed by undergraduate students in the Department of Marine Studies at University of the Aegean. We wish to acknowledge the Municipal Port Fund of Lesvos, Municipality of Lesvos Island, Hellenic Rescue Team, Mytilene

Sailing Club and Mytilene Air Club for their support during our experiment. Funding was provided by Greek State Scholarship Foundation (I.K.Y.) Scholarship Programs, ‘Strengthening Post-Doctoral Research’ Act from the resources of the OP ‘Human Resources Development and Lifelong Learning’ priority axis 6, 8, 9 and co-financed by the European Social Fund–ESF and the Greek government. Deutsche Forschungsgemeinschaft (DFG, German Research Foundation) – Projektnumer 417276871 funding is greatly appreciated. Planet© Dove satellite was made available through the RapidEye Science Archive project ID 00266.

References

- Aoyama, T., 2016. Extraction of marine debris in the Sea of Japan using high-spatial-resolution satellite images. Proceedings Proceedings of SPIE Volume: 9878, Remote Sensing of the Oceans and Inland Waters: Techniques, Applications, and Challenges 9878 987817-987811-987817-987817.
- Cloutis, E.A., 1989. Spectral reflectance properties of hydrocarbons: remote-sensing implications. *Science* 245 (4914), 165–168.
- Cololina, I., Molina, P., 2014. Unmanned aerial systems for photogrammetry and remote sensing: a review. *Isprs J. Photogramm. Remote. Sens.* 92, 79–97.
- Colton Jr., J.B., Knapp, F.D., Burns, B.R., 1974. Plastic particles in surface waters of the Northwestern Atlantic. *Science* 185 (4150), 491–497.
- Cook, K.L., 2017. An evaluation of the effectiveness of low-cost UAVs and structure from motion for geomorphic change detection. *Geomorphology* 278, 195–208.
- Doukari, M., Papakonstantinou, A., Topouzelis, K., 2016. The integration of UAS and structure for motion pipeline for High- Resolution 3D visualization of beach zone topography. Proceedings ISISA Islands of the World XIV Conference 2016 Niss(i) ology and Utopia: back to the roots of Island Studie 1.
- Eltner, A., Baumgart, P., Maas, H.-G., Faust, D., 2015. Multi-temporal UAV data for automatic measurement of rill and interrill erosion on loess soil. *Earth Surf. Process. Landf.* 40 (6), 741–755.
- G20, 2017. Annex to G20 Leaders Declaration: G20 Action Plan on Marine Litter, G20 Summit 2017: Hamburg, Germany (7–8 July), Federal Ministry for the Environment, Nature Conservation, Building and Nuclear Safety. pp. 7.
- Garaba, S.P., Dierssen, H.M., 2018. An airborne remote sensing case study of synthetic hydrocarbon detection using short wave infrared absorption features identified from marine-harvested macro- and microplastics. *Remote Sens. Environ.* 205, 224–235.
- Garaba, S.P., Aitken, J., Slat, B., Dierssen, H.M., Lebreton, L., Zielinski, O., Reisser, J., 2018. Sensing ocean plastics with an airborne hyperspectral shortwave infrared imager. *Environ. Sci. Technol.* 52 (20), 11699–11707.
- Garaba, S.P., Zielinski, O., 2013. Comparison of remote sensing reflectance from above-water and in-water measurements west of Greenland, Labrador Sea, Denmark Strait, and west of Iceland. *Opt. Express* 21 (13), 15938–15950.
- Hooker, S.B., Lazin, G., Zibordi, G., McLean, S., 2002. An evaluation of above- and in-water methods for determining water-leaving radiances. *J. Atmos. Oceanic Technol.* 19 (4), 486–515.
- Hörig, B., Kühn, F., Oschütz, F., Lehmann, F., 2001. HyMap hyperspectral remote sensing to detect hydrocarbons. *Int. J. Remote Sens.* 22 (8), 1413–1422.
- Huth-Fehre, T., Feldhoff, R., Kantimm, T., Quick, L., Winter, F., Cammann, K., van den Broek, W., Wienke, D., Melssen, W., Buydens, L., 1995. NIR - Remote sensing and artificial neural networks for rapid identification of post consumer plastics. *J. Mol. Struct.* 348 (0), 143–146.
- Ivar do Sul, J.A., Costa, M.F., 2014. The present and future of microplastic pollution in the marine environment. *Environ. Pollut.* 185, 352–364.
- Keshava, N., Mustard, J.F., 2002. Spectral unmixing. *IEEE Signal Process. Mag.* 19 (1), 44–57.
- Kou, L., Labrie, D., Chylek, P., 1993. Refractive indices of water and ice in the 0.65- to 2.5- μ m spectral range. *Appl. Opt.* 32 (19), 3531–3540.
- Mace, T.H., 2012. At-sea detection of marine debris: overview of technologies, processes, issues, and options. *Mar. Pollut. Bull.* 65 (1–3), 23–27.
- Mancini, F., Dubbini, M., Gattelli, M., Stecchi, F., Fabbri, S., Gabbianelli, G., 2013. Using unmanned aerial vehicles (UAV) for high-resolution reconstruction of topography: the structure from motion approach on coastal environments. *Remote Sens.* 5 (12), 6880.
- Maximenko, N., Arvesen, J., Asner, G., Carlton, J., Castrence, M., Centurioni, L., Chao, Y., Chapman, J., Chirayath, V., Corradi, P., Crowley, M., Dierssen, H.M., Dohan, K., Eriksen, M., Galgani, F., Garaba, S.P., Goni, G., Griffin, D., Hafner, J., Hardesty, D., Isobe, A., Jacobs, G., Kamachi, M., Kataoka, T., Kubota, M., Law, K.L., Lebreton, L., Leslie, H.A., Lumpkin, R., Mace, T.H., Mallos, N., McGillivray, P.A., Moller, D., Morrow, R., Moy, K.V., Murray, C.C., Potemra, J., Richardson, P., Robberson, B., Thompson, R., van Sebille, E., Woodring, D., 2016. Remote Sensing of Marine Debris to Study Dynamics, Balances and Trends.
- Novelli, A., Tarantino, E., 2015. Combining ad hoc spectral indices based on LANDSAT-8 OLI/TIRS sensor data for the detection of plastic cover vineyard. *Remote. Sens. Lett.* 6 (12), 933–941.
- Papakonstantinou, A., Topouzelis, K., Pavlogeorgatos, G., 2016. Coasline zones Identification and 3D coastal mapping using UAV spatial data. *ISPRS Int. J. Geoinf.* 5 (6), 75.
- PlasticsEurope, 2018. Plastics – the Facts 2017: an Analysis of European Plastics Production, Demand and Waste Data. PlasticsEurope.
- Rezania, S., Park, J., Md Din, M.F., Mat Taib, S., Talaiekhozani, A., Kumar Yadav, K., Kamyab, H., 2018. Microplastics pollution in different aquatic environments and biota: a review of recent studies. *Mar. Pollut. Bull.* 133, 191–208.
- Shammugam, S., SrinivasPerumal, P., 2014. Spectral matching approaches in hyperspectral image processing. *Int. J. Remote Sens.* 35 (24), 8217–8251.
- Plastic Debris in the Ocean: The Characterization of Marine Plastics and Their Environmental Impacts, Situation Analysis Report. In: Thevenon, F., Carroll, C., Sousa, J. (Eds.), .
- Tonkin, T.N., Midgley, N.G., Graham, D.J., Labadz, J.C., 2014. The potential of small unmanned aircraft systems and structure-from-motion for topographic surveys: a test of emerging integrated approaches at Cwm Idwal, North Wales. *Geomorphology* 226, 35–43.
- Vanhellemont, Q., Ruddick, K., 2018. Atmospheric correction of metre-scale optical satellite data for inland and coastal water applications. *Remote Sens. Environ.* 216, 586–597.
- Veenstra, T.S., Churnside, J.H., 2012. Airborne sensors for detecting large marine debris at sea. *Mar. Pollut. Bull.* 65 (1–3), 63–68.